Fermi National Accelerator Laboratory

FERMILAB-CONF-92/11-T
January 1992

NEUTRINO MASSES AND MIXINGS IN SEESAW MODELS WITH QUARK-LEPTON SYMMETRY*

CARL H. ALBRIGHT†
Department of Physics, Northern Illinois University,
DeKalb, Illinois 60115, USA‡
and
Fermi National Accelerator Laboratory,
Batavia, Illinois 60510, USA

ABSTRACT

A summary is presented of the author's attempts in a series of papers to determine the neutrino masses and mixings in seesaw models with three left-handed doublet and three right-handed singlet neutrinos, where the Dirac submatrix exhibits a hierarchical chiral symmetry-breaking structure similar to that for quarks. If one requires depletions of both the solar ν_e and atmospheric ν_μ fluxes, as recently observed by both the Kamiokande and IMB experiments, the right-handed Majorana submatrix must exhibit a hierarchical chiral symmetry-breaking form remarkably similar to that for the Dirac submatrix.

The present highly accurate e^+e^- collider experiments performed in the LEP ring at CERN have revealed[1] at the Z peak that there are just three flavors of light left-handed doublet neutrinos under the $SU(2)_L \times U(1)_Y$ electroweak group. But no information emerges concerning the number of heavy left-handed doublet states, for kinematical reasons, or right-handed isosinglet neutrinos, for electroweak-symmetry reasons. Alternatively, little is known about the number of neutrino mass eigenstates other than that the minimum number is three, whether the neutrinos are Dirac or Majorana,[2] let alone their specific masses and mixings. In the following, we shall assume there are three left-handed doublet and three right-handed singlet neutrinos and present the results from a series of studies[3-5] which seeks to determine the mass and mixing spectrum in a well-defined framework.

1. Seesaw Models with Six Majorana Neutrinos

The lepton mass matrices must then be 6×6 complex symmetric and can be written in terms of the left-handed and right-handed Majorana submatrices $\mathbf{L}_M$ and $\mathbf{R}_M$, in addition to the Dirac submatrices $\mathbf{M}_N$ and $\mathbf{M}_L$, as

$$M_N = \begin{pmatrix} \mathbf{L}_M & \mathbf{M}_N \\ \mathbf{M}_N^T & \mathbf{R}_M \end{pmatrix}, \qquad M_L = \begin{pmatrix} 0 & \mathbf{M}_L \\ \mathbf{M}_L^T & 0 \end{pmatrix} \tag{1}$$

*To appear in *Proceedings of the Workshop on Long-Baseline Neutrino Oscillations* held at Fermilab, 17-20 November 1991
†Research supported in part by NSF Grant No. PHY-8907806 from the National Science Foundation.
‡Permanent address

in the weak flavor bases $\overline{B_L} = \{\overline{\nu'_{iL}},\ \overline{(N'^c_i)_L}\}$, $B_R = \{(\nu'^c_i)_R,\ N'_{iR}\}$ for neutrinos and likewise for the charged leptons. We shall proceed to make the following additional assumptions:

a. No Higgs triplets are present, so $\mathbf{L}_M = 0$.

b. The quark and lepton Dirac matrices exhibit quark-lepton symmetry in a form to be presented below.

c. The nonzero $\mathbf{R}_M$ entries are much larger than the $\mathbf{M}_N$ Dirac entries, so that the well-known seesaw effect[6] is developed; moreover, we shall assume that $\mathbf{R}_M$ has rank three, so that six self-conjugate Majorana neutrino mass states emerge through diagonalization of M_N.

With the above assumptions, the weak charged-current Lagrangian

$$\mathcal{L}_W^{(\pm)} = -\frac{g}{\sqrt{2}}\overline{\nu_{\alpha L}}\gamma^\mu V_{\alpha i}\ell_{iL}W_\mu + h.c. \tag{2}$$

written in the mass basis involves a mixing matrix which is 6×3, as all six neutrino mass eigenstates couple to just three charged-lepton states. Generalized unitarity implies that the sum over row elements of $V_{\alpha i}$ is given by

$$0 \le \sum_{i=1}^{3} |V_{\alpha i}|^2 \le 1 \qquad \text{for each } \alpha = 1,2,...,6 \tag{3a}$$

subject to the restriction

$$\sum_{\alpha=1}^{6} |V_{\alpha i}|^2 = 1 \qquad \text{for each } i = 1,2,3 \tag{3b}$$

With the rank 3 seesaw mechanism operating, the three light Majorana neutrinos nearly saturate the unitarity bound in (3a), so that

$$\sum_{i=1}^{3} |V_{\alpha i}|^2 \simeq \begin{cases} 1, & \alpha = 1,2,3 \\ 0, & \alpha = 4,5,6 \end{cases} \tag{3c}$$

as the heavy Majorana neutrinos effectively decouple from the weak interactions. This is in keeping with the notion that the left-handed flavor states are mainly linear combinations of light neutrino mass eigenstates, while the singlet flavor states are mainly combinations of the massive neutrino states.

In the spirit of grand unification,[7] we assume representative hierarchical chiral symmetry-breaking forms for the Dirac submatrices analogous to the empirical matrices[8] which have been deduced for the quarks on the basis of a top quark mass near 130 - 135 GeV favored by the neutral-current[9] and flavor-changing[10] data:

$$\mathbf{M}_N = \begin{pmatrix} 0 & A_N & A_N \\ A_N & A_N & B_N \\ A_N & B_N & C_N \end{pmatrix}, \qquad \mathbf{M}_L = \begin{pmatrix} 0 & iA'_L & -A'_L \\ -iA'_L & -A'_L & B'_L \\ -A'_L & B'_L & C'_L \end{pmatrix} \tag{4a}$$

Strictly speaking the quark-lepton symmetry between $\mathbf{M}_N$ and the up quark mass matrix and between $\mathbf{M}_L$ and the down quark mass matrix holds only at the grand unification scale. We shall approximate the renormalization effects by adopting the same forms at the low energy scale, rather than assuming equality of the sets of quark and lepton mass matrices. The decisive advantage of this assignment is that we need deal with just three real parameters in each of these matrices, which keeps the complexity of our search manageable without greatly distorting the results. The three charged-lepton parameters are then determined uniquely from the known masses and invariant traces and determinant to be $A'_L = 7.576$ MeV, $B'_L = 0.4181$ GeV and $C'_L = 1.686$ GeV, while the neutrino entries are required to satisfy hierarchical chiral symmetry-breaking conditions[11] for which we assume the inequalities

$$0 < |A_N/C_N| \lesssim 0.2|B_N/C_N| \lesssim 0.04 \tag{4b}$$

The right-handed Majorana submatrix $\mathbf{R}_M$ remains completely unspecified without an explicit theoretical model, but as noted before, we shall assume here it is rank three, so as to give the well-known seesaw mechanism.[6] We now summarize briefly the procedure followed in Refs. 3 - 5 and present the results.

2. Mixing Plane Results for Diagonal $\mathbf{R}_M$

In general $\mathbf{R}_M$ is complex symmetric, but we shall first consider it diagonal and positive real as given by $\mathbf{R}_M = \mathbf{D}_M = diag(D_1,\ D_2,\ D_3)$. From the scaling properties of the seesaw mechanism, if the Dirac parameters A_N, B_N and C_N are scaled by a factor of 10, while D_1, D_2 and D_3 are scaled by a factor of 100, the light masses and mixings remain unchanged; hence for this real diagonal $\mathbf{R}_M$ situation, there are just 5 independent parameters: A_N/C_N, B_N/C_N and the three D_i/C_N's. The squares of the 6×3 mixing matrix elements $V_{\alpha i}$ in the mass basis, where $\alpha = 1-6$, $i = 1-3$, can be calculated from the mass matrices in (1) by a generalization of Jarlskog's projection operator technique[12] as explained fully in Refs. 3 and 4. In doing so, we find the value of $|V_{12}|^2$ is independent of the D_i's and determined only by the ratios A_N/C_N and B_N/C_N. A *minimum* value of $|V_{12}|$ exists such that $\sin^2 2\theta_{12} \sim 4|V_{12}|^2 \geq 0.0193$; replacement of the forms in (4a) by the Fritzsch[11] matrix forms reveals that this lower bound arises from the 90° phase of the 12 element in $\mathbf{M}_L$ and would become weaker and weaker if the phase were reduced toward 0°, corresponding to the disappearance of all CP violation. The lower bound quoted above has interesting implications for the expected solar neutrino capture rates[13] in the experimentally-preferred nonadiabatic Mikheyev, Smirnov and Wolfenstein[14] (MSW) region which translates into a maximum capture rate in gallium of about 25 - 40 SNU in the nonadiabatic region as shown in Fig. 1 from the work[15] of Parke and Walker and Bahcall and Haxton. The preliminary data from the SAGE experiment[16] are quite consistent with this observation.

We now fix $|V_{12}|^2 \simeq \sin^2\theta_{12} = 0.00485$ and adjust $\delta m^2_{12} \equiv m^2_{\nu_2} - m^2_{\nu_1}$ so that the point lies in the narrow allowed nonadiabatic MSW band specified by[17]

$$\delta m^2_{12} \sin^2\theta_{12} \simeq 10^{-8}\ \mathrm{eV}^2 \tag{5}$$

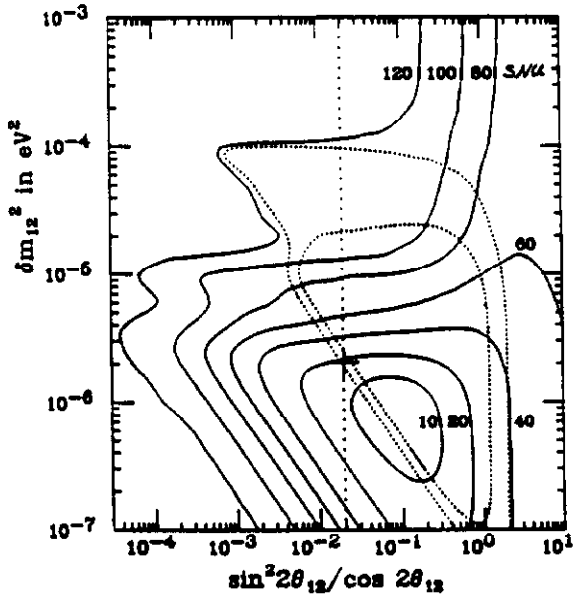

Fig. 1. IsoSNU contours calculated by Parke and Walker[15] for the gallium experiments superimposed on the allowed MSW region indicated by the closely-space dotted points. The vertical dotted line marks the lower bound on $\sin^2 2\theta_{12}$ found in our model. The cross indicates the point held fixed for the remaining figures.

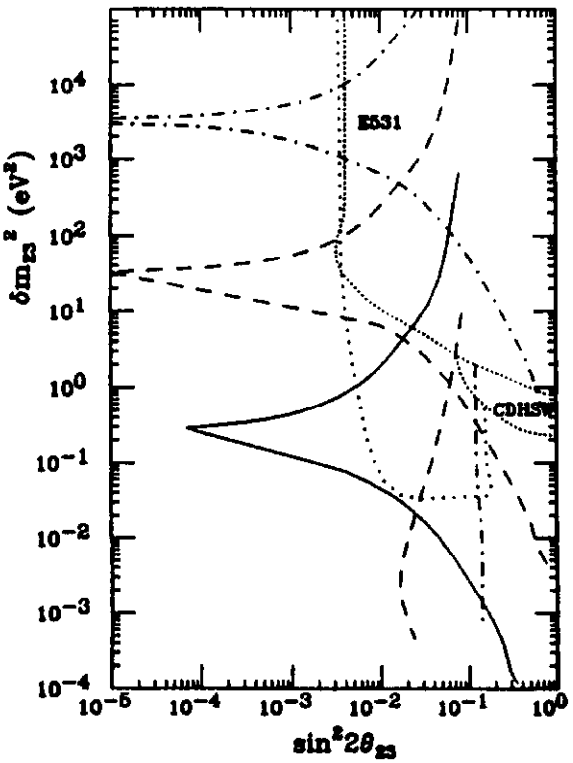

Fig. 2. Contours in the δm_{23}^2 vs. $\sin^2 2\theta_{23}$ plane for fixed $\delta m_{12}^2 = 2.06 \times 10^{-6}$ eV^2 and $|V_{12}|^2 = 0.00485$ in the nonadiabatic MSW region with the curve convention indicated in (6).

i.e., $\delta m_{12}^2 \simeq 2.06 \times 10^{-6}$ eV^2. This is done by scaling the D_i's accordingly, where we choose D_i's in the ratios

$$\begin{array}{lll} (a) & D_1 = 10^2 D_2 = 10^4 D_3 & \text{(upper dot} - \text{dashed curve)} \\ (b) & D_1 = 10 D_2 = 10^2 D_3 & \text{(upper dashed curve)} \\ (c) & D_1 \sim D_2 \sim D_3 & \text{(solid curve)} \\ (d) & 10^2 D_1 = 10 D_2 = D_3 & \text{(lower dashed curve)} \\ (e) & 10^4 D_1 = 10^2 D_2 = D_3 & \text{(lower dot} - \text{dashed curve)} \end{array} \qquad (6)$$

By varying the ratios A_N/C_N and B_N/C_N while holding $|V_{12}|^2$ fixed, one traces out the curves in Fig. 2 corresponding to the D_i ratios of (6) above. Note that we have now plotted the 'noses' more accurately than was done earlier in Refs. 3 and 4. The allowed physical region in the δm_{23}^2 vs. $\sin^2 2\theta_{23}$ plane is then bounded from below by the dotted curve in Fig. 2, if one imposes the hierarchy conditions in (4b). For comparison, the present upper bounds from the E531 experiment[18] at Fermilab and the CDHSW[19] collaboration at CERN are indicated by the closely-spaced dotted curves.

Other fixed points along the MSW nonadiabatic band have been studied[3,4], but the results will not be presented here. We have also looked into the situation where the diagonal form for $\mathbf{R}_M$ is allowed to assume negative values. We then find that the allowed physical region increases considerably by extending downward and to the left, but our most important conclusions to be drawn in section 4 remain unchanged.

3. Mixing Plane Results for Nondiagonal $\mathbf{R}_M$

In Ref. 4 our analysis was generalized to include nondiagonal $\mathbf{R}_M$ by performing orthogonal rotations on the $\mathbf{D}_M$ forms used in Ref. 3,

$$\mathbf{R}_M = R^T(\alpha,\beta,\gamma)\mathbf{D}_M R(\alpha,\beta,\gamma) \tag{7}$$

For this purpose, we selected three points indicated by crosses in Fig. 3(a) lying along each curve obtained previously for the five cases in (6) above, and performed a Monte Carlo analysis by choosing at random 5000 rotations for each point. Fortunately, the values of $|V_{12}|^2$ remain fixed at 0.00485, while the D_i's must be rescaled with each rotation to maintain the same point in the MSW band at $\delta m^2_{12} = 2.06 \times 10^{-6}$ eV^2. The results appear in the form of the scatter plot also illustrated in Fig. 3(a). It is clear from this figure, that while the greater density of points indicating the largest probability lies within the dot-dashed curve obtained in section 2, there are a number of exceptional points outside this boundary which can not be excluded on the basis of our analysis. The results for the 13 mixing plane obtained in a similar fashion are shown in Fig. 3(b). The scatter of points lies much further from the present experimental upper boundary curve than the point suggested by a 17 keV tau neutrino found in several beta decay experiments using solid-state detectors.[20] It is interesting to note that attempts[21] to incorporate the 17 keV neutrino into our hierarchical chiral symmetry-breaking framework with quark-lepton symmetry failed when we replaced $\mathbf{R}_M$ by a rank 2 matrix.

4. Depletion of Atmospheric Muon Neutrino Flux

We now address the issue[5] whether we can simultaneously explain not only the MSW depletion of the solar electron-neutrino flux but also the depletion of the atmospheric muon-neutrino flux. The Kamiokande[22] result is quoted as

$$\frac{(\mu/e)_{data}}{(\mu/e)_{MC}} = 0.61 \pm 0.07 \tag{8a}$$

and has just been confirmed by the IMB group[23] at this Workshop. We simply translate this into the probability that the muon-flavor neutrino produced in the atmosphere by pion decay will remain a muon-flavor neutrino upon detection in the Kamiokande water Cerenkov counter:

$$0.54 \leq \mathrm{Prob}(\nu_\mu \to \nu_\mu) \leq 0.68 \tag{8b}$$

since the probability that the electron-neutrino remains an electron-neutrino is very close to unity. We approximate the three-component oscillation probability by

$$\begin{aligned} \mathrm{Prob}(\nu_\mu \to \nu_\mu) &= 1 - 4\textstyle\sum_{i<j=1}^{3}(V_{i\mu})^2(V_{j\mu})^2 \sin^2 \frac{\delta m^2_{ij}}{4E} L \\ &\simeq 1 - 2(V_{1\mu})^2(V_{3\mu})^2 - 2(V_{2\mu})^2(V_{3\mu})^2 \end{aligned} \tag{9}$$

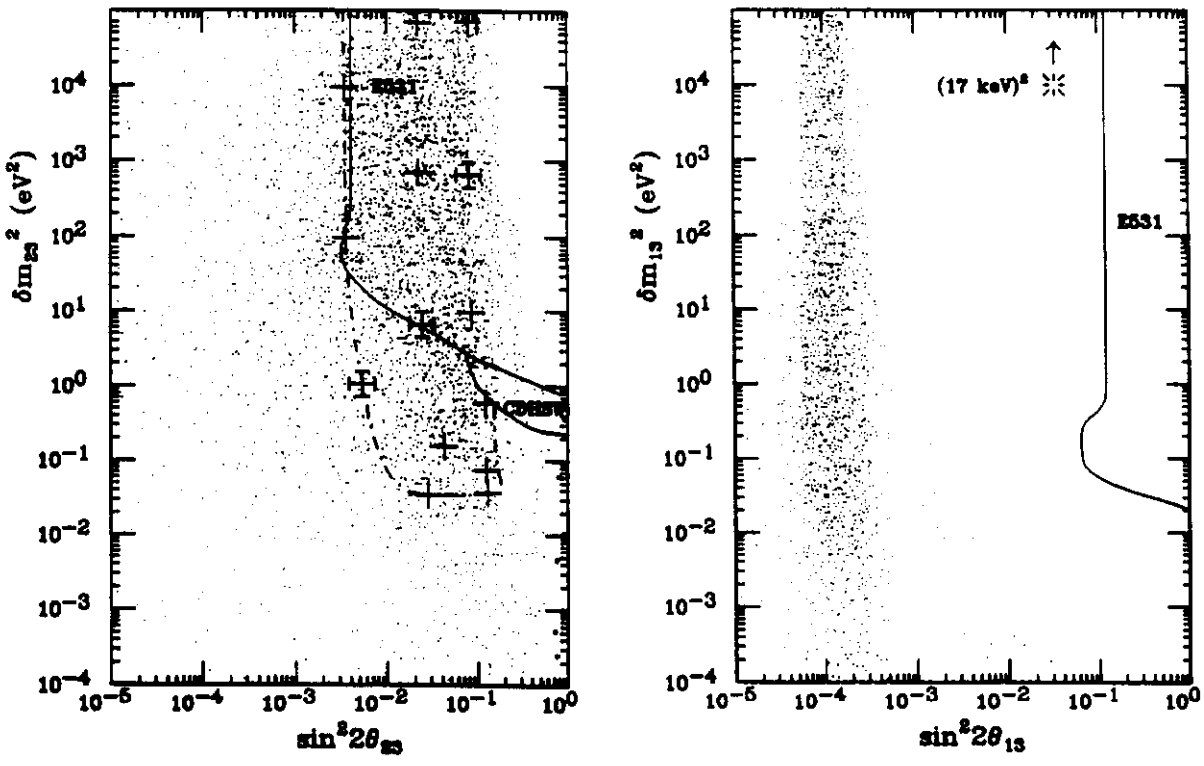

Fig. 3. Scatter plots in the (a) δm^2_{23} vs. $\sin^2 2\theta_{23}$ and (b) δm^2_{13} vs. $\sin^2 2\theta_{13}$ planes obtained by rotating the diagonal $\mathbf{D}_M$ matrices in (6) through Euler angles chosen by 5000 sets of Monte Carlo throws as described in the text. The solid curves represent the present experimental upper limits, while the dot-dashed curve in (a) now corresponds to the hierarchical lower bound in Fig. 2.

since the 12 oscillation length is much longer than the atmospheric production flight-path length. In fact, detailed atmospheric neutrino flux calculations[24] suggest the 13 and 23 oscillations only become important for $\delta m^2_{13} \sim \delta m^2_{23} \gtrsim (0.1 - 2) \times 10^{-3}$ eV^2.

We now use (9) and impose the restriction (8b) on our results for the scatter plot obtained by the Euler rotations explained earlier. The points which survive this cut are indicated by the larger scatter points all located at the lower right-hand edge of Fig. 3(a), below the CDHSW boundary curve and for $\sin^2 2\theta_{23} \gtrsim 0.65$. Of the 60,000 points generated by our Monte Carlo program, just slightly more than 100 pass the probability cut in (8b). Nevertheless, a scan through the mass and mixing output of the points selected shows a clear pattern, from which we can identify the form of $\mathbf{R}_M$ required.

The mixing matrices are all very similar – but very different from the Cabibbo-Kobayashi-Maskawa mixing matrix in the quark case, and in a special but typical case

we find for the light 3×3 sector

$$|V_{\alpha i}|^2 = \begin{pmatrix} 0.99514 & 0.00485 & 0.00001 \\ 0.00367 & 0.76359 & 0.23274 \\ 0.00119 & 0.23156 & 0.76724 \end{pmatrix} \tag{10a}$$

leading, in the standard sign convention, to

$$V = \begin{pmatrix} 0.998 & 0.070 & 0.003e^{-i106^\circ} \\ -0.061 - 0.001i & 0.874 & 0.482 \\ 0.034 - 0.003i & -0.481 & 0.876 \end{pmatrix} \tag{10b}$$

with $\sin^2 2\theta_{23} = 0.711$, $\text{Prob}(\nu_\mu \to \nu_\mu) = 0.64$; the two-component oscillation variable $\sin^2 2\theta_{12}$, determined from the formula for $\text{Prob}(\nu_e \to \nu_e)$ analogous to (9) with all $\sin^2 \frac{\delta m^2_{ij}}{4E} L$ set equal to 0.5, is calculated to be $\sin^2 2\theta_{12} = 0.0194 = 4|V_{12}|^2$ as required. Note the unitary nature of this 3×3 submatrix which is an excellent check on our numerical procedure. The mass matrix parameters for this specific case are $A_N = 30$ MeV, $B_N = 10.8$ GeV and $C_N = 69.1$ GeV, when C_N is scaled relative to the charged lepton and quark mass matrices as noted in Refs. 3 and 4; with the right-handed Majorana mass submatrix then given by

$$\mathbf{R}_M = \begin{pmatrix} 0.0089 & 0.0103 & 0.0464 \\ 0.0103 & 0.0186 & 0.1174 \\ 0.0464 & 0.1174 & 0.8556 \end{pmatrix} \times 10^{15} \text{ GeV} \tag{11a}$$

the mass eigenvalues are found to be

$$\begin{array}{lll} m_1 = 1.53 \times 10^{-11} \text{ eV}, & m_2 = 1.44 \times 10^{-3} \text{ eV}, & m_3 = 0.123 \text{ eV} \\ m_4 = 8.74 \times 10^{10} \text{ GeV}, & m_5 = 8.74 \times 10^{12} \text{ GeV}, & m_6 = 8.74 \times 10^{14} \text{ GeV} \end{array} \tag{11b}$$

In comparison, the CKM mixing matrix deduced for the empirical set of hierarchical chiral symmetry-breaking quark mass matrices[8] yielding a top quark mass near 130 - 135 GeV, which prompted this study, is given by

$$V_{CKM} = \begin{pmatrix} 0.975 & 0.222 & 0.003e^{-i106^\circ} \\ -0.222 & 0.974 & 0.045 \\ 0.011 - 0.003i & -0.044 - 0.001i & 0.999 \end{pmatrix} \tag{10c}$$

The class of models that simultaneously satisfies both the MSW effect for the solar defficiency and the depletion of the atmospheric ν_μ flux has the hierarchical chiral symmetry-breaking structure exhibited in (11a), remarkably similar in form to the Dirac submatrix $\mathbf{M}_N$ in (4a), and more generally is approximately proportional to the matrix

$$\mathbf{R}_M \sim \begin{pmatrix} \tan^2\beta \cos^2\gamma & -\tan^2\beta \sin\gamma \cos\gamma & -\tan\beta \cos\gamma \\ -\tan^2\beta \sin\gamma \cos\gamma & \tan^2\beta \sin^2\gamma & \tan\beta \sin\gamma \\ -\tan\beta \cos\gamma & \tan\beta \sin\gamma & 1 \end{pmatrix} \tag{12}$$

with $\beta \sim 9^o \pm 4^o$ and $\gamma \sim 90^o \pm 40^o$. Thus while the selected points are not statistically significant, we find an intriguing suggestion that some Lagrangian theory may well single out Dirac and right-handed Majorana neutrino mass submatrices which exhibit a similar hierarchical chiral symmetry-breaking form.

In closing we point out that just several acceptable solutions with the simultaneous flux depletions were obtained when the point ($\sin^2\theta_{12} = 0.05$, $\delta m^2_{12} = 2.0 \times 10^{-7}$ eV^2) was chosen in the MSW band. It thus appears that the simultaneous depletion effect limits the allowed region in the nonadiabatic MSW band to the range between the two points (0.00485, 2.06×10^{-6} eV^2) and (0.05, 2.0×10^{-7} eV^2) for this class of models. The cases of negative entries in $\mathbf{D}_M$ of (6) have also been studied but do not change our conclusion above.

References

1. F. Dydak, in *Proceedings of the XXV International Conference on High Energy Physics*, (World Scientific Publishing, Singapore, 1990).
2. See, e.g., C. H. Albright, in Proceedins of the 1991 DPF Conference, Vancouver (to be published); and more generally, B. Kayser, F. Perrier and F. Gibrat-Debu, *The Physics of Massive Neutrinos*, (World Scientific, Singapore, 1989).
3. C. H. Albright, Phys. Rev. D **43**, R3595 (1991).
4. C. H. Albright, Fermilab preprint FERMILAB-PUB-91/182-T, to be published.
5. C. H. Albright, Phys. Rev. D, in press.
6. M. Gell-Mann, P. Ramond and R. Slansky, in "Supersymmetry," edited by P. Van Nieuwenhuizen and D. Z. Freedman (North Holland, 1979); T. Yanagida, Prog. Theor. Phys. B **315**, 66 (1978).
7. R. Johnson, S. Ranfone and J. Schechter, Phys. Lett. **179B**, 355 (1986); G. Lazarides and Q. Shafi, Nucl. Phys. B **350**, 179 (1991); I. Antoniadis, J. Ellis, J. S. Hagelin and D. V. Nanopoulos, Phys. Lett.B **231**, 65 (1989).
8. C. H. Albright, Phys. Lett. B **246**, 451 (1990); Fermilab preprint FERMILAB-CONF-90/104-T, contribution to the XXV International High Energy Physics Conference, Singapore (1990), unpublished.
9. J. Ellis and G. L. Fogli, Phys. Lett. B **232**, 139 (1989); P. Langacker, Phys. Rev. Lett. **63**, 1920 (1989); V. Barger, J. L. Hewett and T. G. Rizzo, Phys. Rev. Lett. **65**, 1313 (1990); J. L. Rosner, Phys. Rev. D **42**, 3107 (1990).
10. Cf., eg., C. H. Albright, in Proceedings of the XXV Int. HEP Conf., Singapore (World Scientific, 1990); and references therein.
11. H. Fritzsch, Phys. Lett. **70B**, 436 (1977); **73B**, 317 (1978); **166B**, 423 (1986).
12. C. Jarlskog, Phys. Rev. D **35**, 1685 (1987); D **36**, 2138 (1987); C. Jarlskog and A. Kleppe, Nucl. Phys. B **286**, 245 (1987).
13. R. Davis et al., Phys. Rev. Lett. **20**, 1205 (1968); in *Neutrino '88*, ed. J. Schnepp et al. (World Scientific, 1988); K. Hirata et al., Phys. Rev. Lett. **65**, 1297, 1301 (1990).
14. S. P. Mikheyev and A. Yu Smirnov, Sov. J. Nucl. Phys. **42**, 913 (1986); Sov. Phys. JETP **64**, 4 (1986); Nuovo Cimento **9C**, 17 (1986); L. Wolfenstein, Phys. Rev. D **17**, 2369 (1978); Phys. Rev. D **20**, 2634 (1979).

15. S. J. Parke and T. P. Walker, Phys. Rev. Lett. **57**, 2322 (1986); J. N. Bahcall and W. C. Haxton, Phys. Rev. D **40**, 931 (1989).
16. V. N. Gavrin, in Proceedings of the XXV Int. HEP Conf., Singapore (World Scientific, 1990); A. I. Abazov et al., Phys. Rev. Lett. **67**, 3332 (1991).
17. E. W. Kolb, M. S. Turner and T. P. Walker, Phys. Lett. **175B**, 478 (1986); S. P. Rosen and S. M. Gelb, Phys. Rev. D **34**, 969 (1986); J. N. Bahcall and H. A. Bethe, Phys. Rev. Lett. **65**, 2233 (1990).
18. N. Ushida et al., Phys. Rev. Lett. **57**, 2897 (1986).
19. F. Dydak et al., Phys. Lett. B **134**, 281 (1984).
20. J. J. Simpson, Phys. Rev. Lett. **54**, 1891 (1985); J. Simpson and A. Hime, Phys. Rev. D **39**, 1825 (1989); A. Hime and J. J. Simpson, Phys. Rev. D **39**, 1837 (1989); B. Sur et al., Phys. Rev. Lett. **66**, 2444 (1991); A. Hime and N. A. Jelley, Phys. Lett. B **257**, 441 (1991); I. Zlimen et al., Ruder Boskovic Institute preprint 11-9/90 LEI.
21. C. H. Albright, Fermilab preprint FERMILAB-PUB-91/29-T, to appear in Phys. Rev. D.
22. K. S. Hirata, et al., Phys. Lett. B **205**, 416 (1988); T. Kajita, in *Singapore '90*, (World Scientific).
23. D. Casper et al., Phys. Rev. Lett. **66**, 2561 (1991); S. Dye, in these proceedings.
24. S. Midorikawa, M. Honda and K. Kasahara, U. of Tokyo preprint ICRR-Report-243-91-12.